Can the updip limit of frictional locking on megathrusts be detected geodetically? Quantifying the effect of stress shadows on near-trench coupling

Lindsey, Eric Ostrom; Bradley, Kyle; Hubbard, Judith; Mallick, Rishav; Hill, Emma Mary; Almeida, Rafael

2018

Almeida, R., Lindsey, E. O., Bradley, K., Hubbard, J., Mallick, R., & Hill, E. M. (2018). Can the Updip Limit of Frictional Locking on Megathrusts Be Detected Geodetically? Quantifying the Effect of Stress Shadows on Near-Trench Coupling. Geophysical Research Letters, 45(10), 4754-4763. doi:10.1029/2018GL077785

https://hdl.handle.net/10356/89817

https://doi.org/10.1029/2018GL077785

AGU100 ADVANCING EARTH AND SPACE SCIENCE

Geophysical Research Letters

RESEARCH LETTER
10.1029/2018GL077785

Key Points:
- Frictionally locked portions of megathrusts create an updip stress shadow, which prevents shallow megathrusts from creeping regardless of frictional behavior
- Modeling the shallow thrust as an end-member free-slipping crack, the expected creep rate is below data resolution even in well-instrumented convergent margins
- Many geodetic models commonly show low to zero coupling at the trench and thus may underestimate seismic and tsunami hazard of the shallow fault

Supporting Information:
- Supporting Information S1

Correspondence to:
E. O. Lindsey,
elindsey@ntu.edu.sg

Citation:
Almeida, R., Lindsey, E. O., Bradley, K., Hubbard, J., Mallick, R., & Hill, E. M. (2018). Can the updip limit of frictional locking on megathrusts be detected geodetically? Quantifying the effect of stress shadows on near-trench coupling. *Geophysical Research Letters*, *45*, 4754–4763. https://doi.org/10.1029/2018GL077785

Received 5 MAR 2018
Accepted 7 MAY 2018
Accepted article online 15 MAY 2018
Published online 28 MAY 2018

Can the Updip Limit of Frictional Locking on Megathrusts Be Detected Geodetically? Quantifying the Effect of Stress Shadows on Near-Trench Coupling

Rafael Almeida[1], Eric O. Lindsey[1], Kyle Bradley[1], Judith Hubbard[1,2], Rishav Mallick[1,2], and Emma M. Hill[1,2]

[1]Earth Observatory of Singapore, Nanyang Technological University, Singapore, [2]Asian School of the Environment, Nanyang Technological University, Singapore

Abstract The updip limit of the seismogenic zone of megathrusts is poorly understood. The relative absence of observed microseismicity in such regions, together with laboratory studies of friction, suggests that the shallow fault is mostly velocity strengthening, and likely to creep. Inversions of geodetic data commonly show low to zero coupling at the trench, reinforcing this view. We show that the locked, downdip portion of the megathrust creates an updip stress shadow that prevents the shallow portion of the fault from creeping at a significant rate, regardless of its frictional behavior. Our models demonstrate that even if the shallowest 40% of the fault is frictionally unlocked, the expected creep at the fault tip is at most 30% of the plate rate, often within the uncertainties of surface geodetic measurements, and below current resolution of seafloor measurements. We conclude that many geodetic models significantly underestimate the degree of shallow coupling on megathrusts, and thus seismic and tsunami hazard.

Plain Language Summary When one tectonic plate dives beneath another, the fault between them is called a megathrust. The shallow part of these faults is not well understood. Generally, it is thought that if this area is pushed, it will freely slip (and will not store energy that would be released as earthquakes). Researchers make models of megathrusts using GPS measurements to determine which parts of it are slipping and which are not (which means they are storing energy that will be released as earthquakes). These models are not well constrained far from the GPS measurements, and in many areas it is difficult to make measurements near the shallow megathrust because they are under the ocean. We use a simple model that considers the forces acting on the fault to show that if the deeper megathrust is not slipping, then it will act as a buffer to prevent the shallow part from moving. We compare our model to megathrusts with many measurements in Japan and Nepal and show that the GPS data cannot tell us if the shallow fault is stuck together by friction or not. This is important because the behavior of the shallow fault affects potential earthquake size and tsunami risk.

1. Introduction

The largest known earthquakes occur at convergent margins, where gently dipping megathrust faults extend deep into Earth (Figure 1). In regions with geodetic data, the distribution of deep interseismic creep (Table 1) on these megathrusts can be estimated through a kinematic inversion for slip rate deficit, or kinematic coupling ratio (hereafter referred to as coupling; e.g., Bürgmann et al., 2005; Chlieh et al., 2008, 2011, 2014; Loveless & Meade, 2016; Metois et al., 2013; Xue et al., 2015). This result is then used to forecast the future coseismic and tsunamigenic behavior of the fault (e.g., Kaneko et al., 2010; Loveless & Meade, 2011; Metois et al., 2013; Moreno et al., 2010).

Many geodetic inversions show low or zero coupling near the trench, where there is limited model resolution (e.g., Chlieh et al., 2008, 2014; Loveless & Meade, 2010; McCaffrey, 2014; Nocquet et al., 2017). This is consistent with a general view that shallow faults are velocity strengthening (e.g., Byrne et al., 1988; Ikari et al., 2009; Marone & Scholz, 1988; Wu et al., 1975) and therefore must creep under applied stress. However, the shallow parts of megathrusts can also be seismogenic (e.g., Hubbard et al., 2015), as evidenced by tsunami earthquakes and shallow slow-slip events. Slip models of the 2010 Mentawai tsunami earthquake (Hill et al., 2012; Yue et al., 2014) suggest that maximum slip occurred adjacent to the trench, an area previously inferred to be creeping interseismically (Chlieh et al., 2008). Shallow slow-slip events (e.g., Saffer & Wallace, 2015;

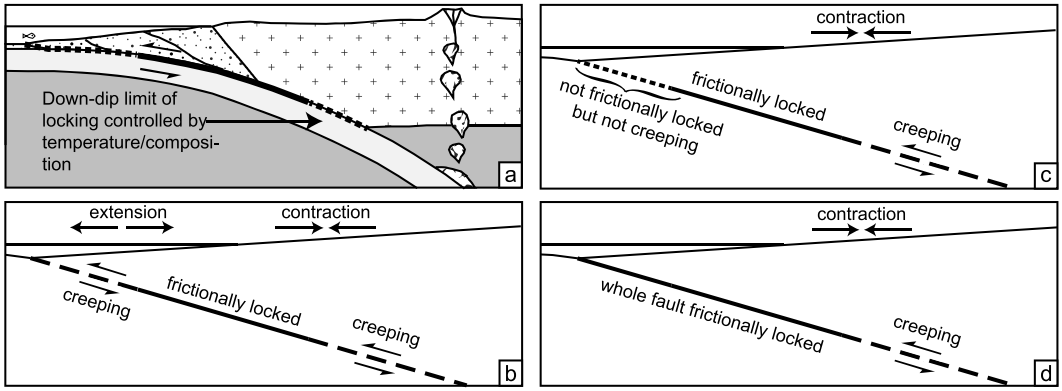

Figure 1. (a) Schematic representation of a subduction zone. Dotted pattern represents the accretionary prism, cross pattern represents arc crust, light gray represents oceanic crust, and dark gray is mantle (modified from Hyndman et al., 1997); (b–d) Alternative models for frictional properties of the shallow megathrust. (b) The shallow fault creeps during the interseismic period, representing a low coupling region. (c) The shallow megathrust is not frictionally locked but does not move because it is located in the stress shadow of the deeper, frictionally locked part of the fault. (d) The whole fault is frictionally locked. Geodetic data cannot distinguish (c) from (d) (modified from Wang & Dixon, 2004).

Wallace et al., 2016, 2017) represent transient behaviors where the fault releases accumulated stress episodically and have been observed to occur in several subduction zones, but their global prevalence remains uncertain (Saffer & Wallace, 2015).

These apparent contradictions highlight our limited understanding of the interseismic behavior of the shallow megathrust. In places without offshore geodetic data, the model resolution for the shallowest part of subduction megathrusts (far from land-based stations) is nearly zero. Therefore, studies commonly adopt regularization techniques to extend the model prediction to the trench. In addition to Laplacian smoothing, one common approach is to minimize the moment accumulation rate; this penalizes high values of coupling near the trench (e.g., Chlieh et al., 2014). However, this approach overlooks the existence of a "stress shadow" updip of locked fault patches (Bürgmann et al., 2005; Hetland & Simons, 2010; Wang & Dixon, 2004). If the megathrust is frictionally locked at any location and therefore fully coupled (i.e., the hanging wall is not moving relative to the footwall), then the megathrust updip of this location will experience a smaller stressing

Table 1
Nomenclature

Term	Definition
Kinematic coupling ratio or slip rate deficit	This is a kinematic term that describes the velocity of the hanging wall of the megathrust relative to the footwall. It thus refers only to the estimated slip rate on the fault and not to the fault's response to stress. Because coupling is often confused with locking, we prefer the more clearly kinematic term slip rate deficit, which can be used interchangeably with coupling. The kinematic coupling ratio or slip rate deficit ratio is the ratio between the interseismic slip rate on a fault patch and the known plate convergence rate.
Creep	Creep on a fault represents any slip that does not occur during the coseismic phase of an earthquake. This can occur during the postseismic or interseismic period. For a given fault patch, the slip rate deficit plus the creep rate equals the local plate convergence rate. Here we use the term creep to refer primarily to interseismic creep.
Locking	A mechanical term referring to the response of a fault to applied stress (Scholz, 1998). To make the distinction from the kinematic description more clear, in this text we use the term frictional locking. The frictional stability of a fault is commonly described using the rate- and state-dependent frictional model (Dieterich, 1981; Ruina, 1983; Scholz, 1998). In the simplest framework, a fault patch that is velocity strengthening becomes stronger as the velocity at which it slips is increased, and it therefore undergoes creep and cannot nucleate earthquakes (i.e., the fault is frictionally unlocked, and if an applied stress exceeds its strength, it will slip via creep). A fault patch that is velocity weakening will become weaker as the slip velocity increases and undergoes stick-slip sliding; such a patch can nucleate earthquakes (i.e., the fault is frictionally locked and slips coseismically; Scholz, 1998). The frictional stability of a fault is unrelated to its strength, which is determined by its static friction, and instead refers to the amount of strain it can accumulate before slipping (Scholz, 1998).

Note. The terms "locking" and "coupling" have long been used interchangeably in the literature (e.g., Lay & Schwarz, 2004; Wang & Dixon, 2004). To avoid confusion, we briefly define the terms as used here.

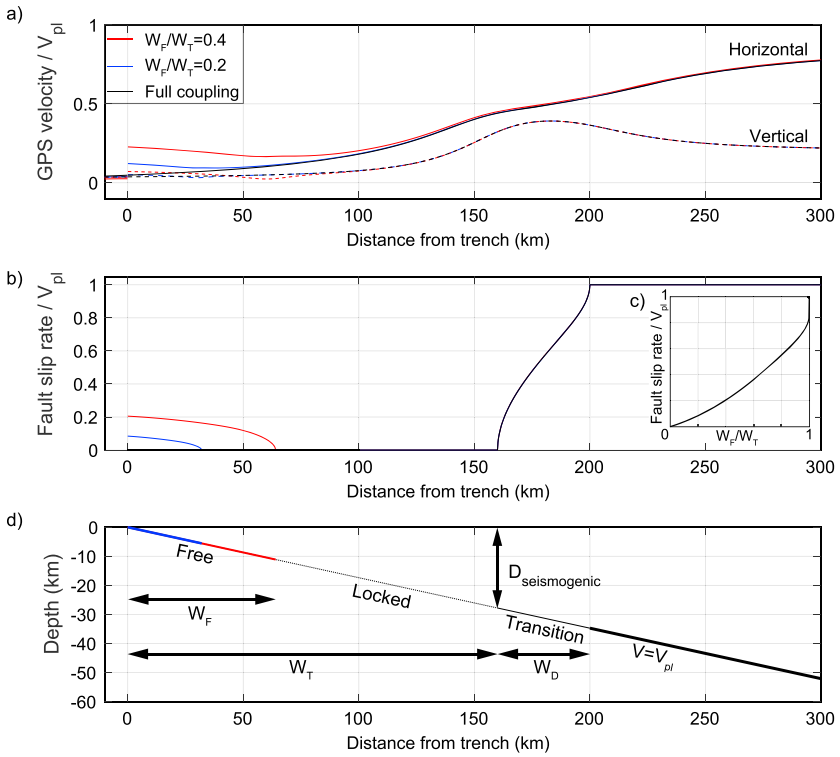

Figure 2. Model setup and results with representative scenarios with W_F/W_T = 0, 0.2, and 0.4. (a) Horizontal (solid) and vertical (dashed) velocities measured at the surface, as a ratio relative to the downgoing plate velocity; (b) fault slip rates relative to the downgoing plate velocity; (c) inset showing the creep rate at the fault tip for all values of the creeping width W_F/W_T; (d) model setup illustrating the relation between the width of fault that is freely slipping (W_F), the total width of the fault (W_T), and the width of the downdip transition zone (W_D). W_F/W_T represents the proportion of the fault above the seismogenic depth that is frictionally unlocked.

rate; that is, it lies within a "stress shadow" (Figure 1). A significant rate of creep updip of this location would require interseismic extension of the hanging wall at a rate related to the change in creep rate (Wang & Dixon, 2004). The location of this extensional strain in a typical subduction zone would be underwater, in the poorly resolved portion of geodetic models, and the driving stress that could cause such extension within the overall compressive regime of a subduction zone is not clear. Further, geologic evidence for extension in accretionary prisms (e.g., Becel et al., 2017; Kodaira et al., 2012) has been interpreted as a consequence of coseismic ruptures of the whole megathrust that result in dynamic effects such as shallow coseismic overshoot, static stress changes, or near-surface effects, and not reflective of interseismic behavior of the megathrust (e.g., Ide et al., 2011; Li et al., 2014; Xu et al., 2016).

This leads us to pose the question: if the shallow megathrust is frictionally unlocked but located in a stress shadow, to what degree can it creep? Here we use a boundary element method to quantify the maximum rate of shallow creep under a variety of conditions. We find that the fault tip cannot slip at a rate approaching the plate velocity under any reasonable set of assumptions. Furthermore, the geodetic signal distinguishing this unlocked-but-not-creeping case from a fully frictionally locked fault is likely too small to be measurable with current techniques. If the shallow megathrust cannot creep during the interseismic period, it must slip either during or soon after earthquakes, and therefore, this question has major implications for estimates of seismic and tsunami hazards, as well as the potential for shallow nucleation of earthquakes.

2. Model and Results

We adopt a two-dimensional physics-based model of a planar fault assuming that there is no variation in fault properties along strike (Figure 1); in a later section, we extend this model to three dimensions to address the effect of along-strike variations. The fault has a fully locked patch in the center of the seismogenic zone.

Above and below this locked area, the fault slips under a zero stressing rate condition (i.e., the fault is considered to have reached its frictional yield strength, and will slip in response to any applied stress). Fault slip is considered as continuous, time-invariant creep. We refer to the unlocked updip portion of the fault as the frictionally unlocked or "free" width, W_F, presented as a ratio to the total fault width, W_T, down to the base of the seismogenic zone (Figure 2). The fault is driven from the far field at a stressing rate determined for each patch such that the whole fault would creep at the long-term rate if the entire fault were frictionally unlocked ($W_F/W_T = 1$). We implement the model using a boundary element method with analytic solutions for displacement and stressing rate (Okada, 1992); a detailed description is found in supporting information Text S1.

We consider a planar fault with a dip of 10°, which is steeper than the shallow megathrust in many convergent margins (e.g., Hubbard et al., 2015) but similar to wedge angles inferred from critical taper theory, commonly ~8–10° (Davis et al., 1983). We define a 40 km-wide transition zone (W_D) at the base of the model, where the fault is frictionally unlocked (no stress accumulation) and the modeled slip rate increases from zero to the plate convergence rate (Figure 2).

We choose the updip and downdip boundaries of the locked patch to correspond with temperatures where the frictional behavior of the fault is thought to change: 80–100°C and 350°C, respectively (Blanpied et al., 1995; Hyndman et al., 1997; Marone, 1998; Scholz, 1988, 1998; Stesky et al., 1974). The shallow megathrust has an approximately linear geothermal gradient, consistent with subduction zone thermal models (Syracuse et al., 2010), so for a planar fault the ratio W_F/W_T can be calculated from the ratio of the two transition temperatures, which yields a value of $W_F/W_T = 0.23–0.29$. However, this simplification neglects plate curvature, which would increase W_F/W_T. Thus, we consider two representative cases, $W_F/W_T = 0.2$ and 0.4 (Figure 2). The results show low creep rates: for the first case, creep does not reach more than 10% of the plate rate, while for the second, it reaches 20% of the long-term rate at the fault tip; this corresponds to a coupling of 0.8. The expected geodetic signal for each case is shown in Figure 2a; like the fault slip rate, the surface velocity near the trench remains small for both models.

To test the wide applicability of our model, the shallow creep rate at the fault tip for all possible values of W_F/W_T between 0 (fully locked) and 1 (fully unlocked) is shown in Figure 2c. Generally, the shallow creep rate increases with W_F/W_T but remains below the 1:1 line for all models. We show the effect of varying the fault dip and the deep transition zone width W_D in supporting information Figure S1. Fault dip has a moderate impact, due to its effect on the proximity of the free surface, which reduces the transfer of stress to the shallow wedge, but even for a dip of 15°, the creep rate at the fault tip does not exceed 30% of the plate convergence rate when $W_F/W_T = 0.4$. We vary the deep transition zone width W_D/W_T between 0 and 1 and find that the effect of W_D on the shallow creep rate is negligible.

We emphasize that the model treats the shallow portion of the fault as a freely slipping crack and thus predicts maximum creep rates. If the shallow fault has variable strength or some small locked patches, the resulting slip rate would be even lower. However, numerous geodetic inversions propose a scenario in which the fault is fully uncoupled (i.e., creeping at the full long-term rate) at the trench (e.g., Chlieh et al., 2008, 2014; McCaffrey, 2014; Nocquet et al., 2017), a scenario we show in Figure S2 (dashed line). The results shown here demonstrate that in such a case, the resultant stressing rate on the shallow part of the fault is negative, representing a release of stored energy and thus inconsistent with long-term interseismic loading of the fault.

3. Comparison to Observational Data

We compare our model predictions to geodetic observations from two well-instrumented convergent margins: the Himalayan megathrust in central Nepal and the Nankai subduction zone in Japan. These are two of the best examples of megathrusts where geodetic velocities are available close to the fault tip—surface GPS observations in Nepal and seafloor geodetic observations in Japan.

In Nepal, the interseismic geodetic velocity field has been measured across the entire megathrust, and models fitting the data show that it is fully coupled to the surface (Ader et al., 2012; Grandin et al., 2012; Jackson & Bilham, 1994; Stevens & Avouac, 2015). We select GPS data from a global compilation (Kreemer et al., 2014) within a 200-km-wide profile in central Nepal (Figure S3), project the component of the horizontal velocities normal to the frontal fault, and plot it against a suite of possible 2-D models in Figure 3a. We assume a dip of 10° and a downdip locking transition between 110 and 150 km north of the surface trace of the frontal thrust

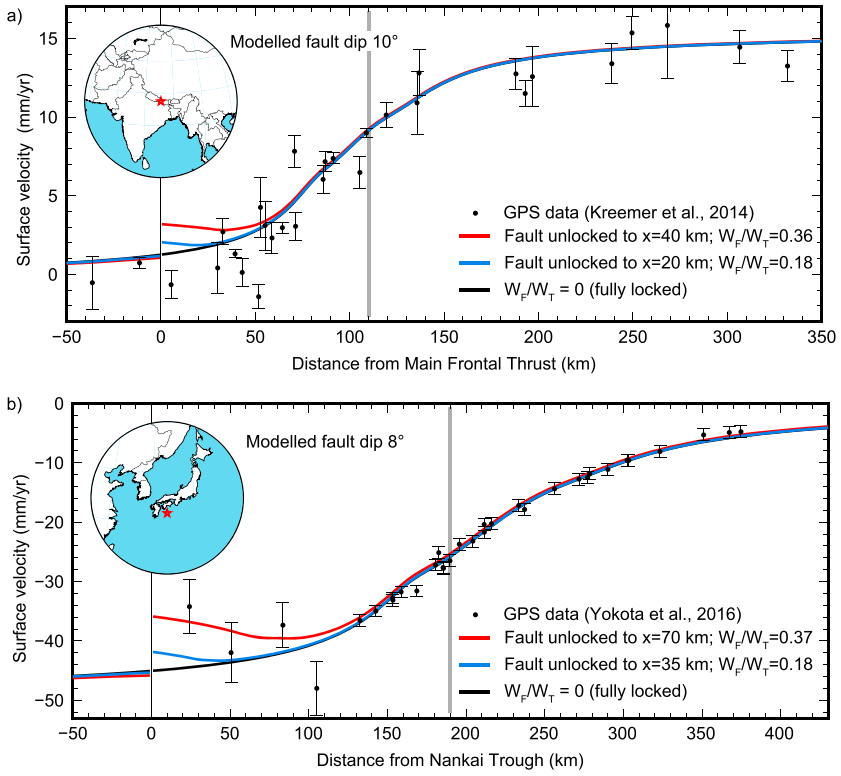

Figure 3. Comparison of horizontal geodetic velocities to model results showing W_F/W_T = 0, 0.18, and 0.36. (a) Data from Nepal (Kreemer et al., 2014) are horizontal velocities perpendicular to smoothed strike of the Main Himalayan Thrust (MHT) (015°); (b) data from Nankai (Yokota et al., 2016) are horizontal velocities perpendicular to the trench (330°). Gray vertical lines show location of downdip edge of locking in each model. The reference frame is India fixed in (a) and Eurasia fixed in (b). Data used to construct these profiles are shown in map view in Figures S3 and S4.

(i.e., the Main Frontal Thrust) (Pandey et al., 1995), similar to values used by other studies in the region (e.g., Ader et al., 2012; Bettinelli et al., 2006; Stevens & Avouac, 2015). Based on thermal models of the megathrust, the fault should reach a temperature of 80°C at 4–5 km depth or 22–28 km from the frontal fault (which we consider analogous to the trench in a subduction zone; Ader et al., 2012; Herman et al., 2010). We use these values to estimate the potentially creeping portion of the Main Himalayan Thrust (MHT) and obtain W_F/W_T = 0.2. If we consider the updip limit of the Gorkha rupture as the maximum extent of the frictionally locked portion of the fault, then W_F/W_T = 0.4, although we note that almost no afterslip has been observed updip of the Gorkha earthquake in 2015, suggesting that this part of the fault is velocity weakening (e.g., Mencin et al., 2016; Zhao et al., 2017). Our model result shows a maximum of 2 mm/year of creep on the tip of the fault (Figure 3a), similar to the scatter in the geodetic measurements. Thus, even for a subaerial wedge, the geodetically derived interseismic velocity field cannot be used to reliably infer the frictional properties of its shallow portion.

Fault properties in subduction zones may be different from those in continental collision zones, particularly due to the availability of fluids, which may alter both the mineralogy of the downgoing sediments and the seismogenic properties of the megathrust (e.g., Saffer, 2017). Seafloor geodetic observations at subduction zones are limited due to cost and logistics, and the errors in such measurements are typically an order of magnitude larger than on land, although the rates of convergence are also typically higher (DeMets et al., 2010).

We consider the case of the Nankai subduction zone offshore Japan, using both land-based and seafloor geodetic data reported by Yokota et al. (2016). We select data within a 100-km-wide profile centered on the western half of the island of Shikoku (Figures 3b and S4). We project the trench-normal component of the horizontal velocities along an azimuth of 330°, consistent with the mean local slip directions of

earthquakes (though there are few earthquakes and the scatter is large), and use a megathrust dip of 8°, based on the Slab1.0 model (Hayes et al., 2012). We conducted a simple grid search and find that the model best fits the data with a wide downdip transition zone between 190 and 290 km from the trench, and a convergence rate of 55 mm/year (Figure 3b). In the Nankai Trough, the updip limit of the locked megathrust has been proposed to be located 40 km from the trench ($W_F/W_T = 0.21$) based on estimates of low-grade metamorphic reaction conditions (Moore & Saffer, 2001). As with Nepal, we use three models to illustrate a range of scenarios: $W_F/W_T = 0$ (fully locked), $W_F/W_T = 0.2$, and $W_F/W_T = 0.4$. Our models show a pattern similar to Nepal, with creep rates of up to a maximum of 10 mm/year at the fault tip—again, close to the measurement uncertainty of seafloor geodesy and highlighting the difficulty of using geodetic inversions for interseismic coupling to infer the frictional properties of the shallow megathrust.

4. Discussion

Our results show that if the downdip part of a megathrust is locked continuously along strike, the resulting stress shadow will prevent significant shallow creep updip, regardless of the mechanical properties of the shallow fault. Therefore, purely kinematic descriptions of slip rate deficit on a megathrust are not sufficient to discriminate the fault's frictional properties.

Our two-dimensional model is representative of convergent margins with continuous along-strike locking of the deep megathrust over a distance greater than their width. We do not consider along-strike variations in frictional locking in detail, which can result in higher creep rates of the shallow megathrust near the edges of locked patches (e.g., Hetland & Simons, 2010). This effect is difficult to quantify concisely, but we illustrate it with one realization of a three-dimensional model in Figure S4, which shows that even for an isolated locked patch, the kinematic coupling ratio updip of the locked area remains above 0.5, with most of the area above 0.75 if the patch is wider than its depth.

4.1. Frictional Properties of the Shallow Megathrust

The seismogenic properties of the downdip megathrust have been studied extensively (e.g., Fitch & Scholz, 1971; Hyndman, 2013; Hyndman et al., 1997; Hyndman & Wang, 1993; Savage, 1983; Tichelaar & Ruff, 1993), but there still is significant uncertainty about the frictional properties of the shallow megathrust (e.g., Lay & Schwarz, 2004; Schmalzle et al., 2014; Wang & Dixon, 2004). Following the 2011 Tohoku-Oki earthquake, which exhibited large amounts of slip at the trench (e.g., Kido et al., 2011; Sun et al., 2017), there has been renewed interest in defining the seismogenic potential of the shallowest parts of megathrusts.

One long-standing model for megathrust behavior is that the fault interface is seismogenic between ~10 to ~30 km depth, with downdip and updip limits of frictional locking bounding the seismogenic zone (Hyndman et al., 1997). Various mechanisms have been proposed to control the location of the updip limit: the onset of velocity strengthening (or stable) frictional behavior in quartzo-feldespathic rocks at temperatures below 80°C (Blanpied et al., 1995); the pressure-dependent frictional transition between velocity strengthening unconsolidated fault gouge and deeper, mature fault zones (Byrne et al., 1988; Marone & Scholz, 1988); the phase transition in clays between illite and smectite in fault gouge (Hyndman et al., 1997; Vrolijk, 1990); and the onset of a series of phase transitions and diagenetic processes that change fluid availability and pressure (Moore & Saffer, 2001; Moreno et al., 2014).

The lack of shallow earthquakes in this region has also commonly been used to infer a change in fault properties at shallow depths (e.g., Marone & Scholz, 1988; Schwarz & DeShon, 2007), but our results suggest instead that this may simply reflect the absence of significant loading stresses. This highlights the key problem encountered when implying direct links between kinematic and mechanical properties of a fault: even though a fault may be frictionally unlocked, if there is no driving force, it will not move and therefore be coupled. Furthermore, observations of shallow creep following earthquakes on terrestrial thrust faults are rare (e.g., Copley & Reynolds, 2014).

The shallowest part of the megathrust is often interpreted as a series of asperities embedded in a creeping or conditionally stable medium, located updip of a mostly locked fault area (e.g., Lay et al., 2012; Lay & Kanamori, 1981). Geodetic studies of subduction zones seem to reinforce this model by estimating patches of high coupling, or high slip rate deficit, surrounded by regions of interseismic creep, despite having limited or no resolution near the trench. These highly coupled "asperities" tend to coincide with regions where there is higher

model resolution (e.g., Konca et al., 2008; Xue et al., 2015), with creeping areas corresponding to regions with little or no model resolution. In fact, these shallow variations are commonly an artifact of the modeling procedure, which either assumes zero coupling at the trench (e.g., Loveless & Meade, 2010; Xue et al., 2015) or includes a minimization of the moment deficit rate, which causes areas with low model resolution to default to fully creeping (e.g., Chlieh et al., 2008, 2014; Konca et al., 2008; Perfettini et al., 2010). Some models may be further biased by problems such as poorly known incoming plate motions and the partitioning of convergence onto faults located within the upper plate (Bradley et al., 2017; Chlieh et al., 2008; McCaffrey, 1991). Where existing geodetic networks have been enhanced by the addition of offshore sites, they have largely failed to show evidence for low coupling near the trench (e.g., Gagnon et al., 2005; Yokota et al., 2016).

4.2. Slip Budget Throughout the Seismic Cycle

Regardless of its frictional properties, our results indicate that the shallow megathrust above a locked zone most likely does not undergo significant interseismic creep. This means that the accumulated slip deficit must be released either coseismically or postseismically. Which of these two is dominant depends on the frictional properties of the fault: velocity weakening behavior would induce larger coseismic slip, while velocity strengthening behavior would result in more postseismic deformation. In the case of coseismic release, the resultant earthquake would be larger than expected, if the shallow megathrust is assumed to be creeping, and will represent an increased hazard.

The accumulated strain over several earthquake cycles, however, would be largely indistinguishable between these cases, making it difficult to infer mechanical properties of the megathrust from observed thrust structures in the accretionary wedge. Thus, in the absence of locally instrumented earthquakes, neither geologic nor interseismic geodetic data are well suited to predict the coseismic behavior of the shallow megathrust (Bilek & Lay, 2002), with the possible exception of extensional structures in the shallow wedge, which may indicate shallow coseismic rupture (e.g., Geersen et al., 2018).

One possible indicator of the frictional properties of the megathrust may be the observed spatial variation in the frequency content of seismic ruptures. The shallow parts of megathrust ruptures are commonly depleted in high-frequency radiation (Denolle et al., 2015; Huang et al., 2012; Lay et al., 2012; Yao et al., 2013; Yue et al., 2016), which has been interpreted to be a consequence of rupture dynamics. Future work in this area, particularly with realistic dynamic rupture simulations, may help elucidate the origin of this phenomenon.

4.3. Implications for Seafloor Geodesy

Our models suggest that interseismic creep rates on most shallow megathrusts are too low to be detected by current seafloor instruments. However, these instruments can still improve our understanding of shallow megathrusts if they are placed in areas where the signal is more likely to be large. We suggest three cases. First, if the downdip area is not locked, the strain gradient in the shallow megathrust will be high. For example, limited land-based data from the island of Java suggest that the Sunda megathrust there may be mostly uncoupled (Abercrombie et al., 2001; Grevemeyer & Tiwari, 2006; Scholz & Campos, 1995), but tsunami earthquakes in 1994 and 2006 (Abercrombie et al., 2001; Ammon et al., 2006) suggest that the updip portion may be velocity weakening. Second, if the updip part of the megathrust is not coupled, there should be an abrupt step in horizontal velocities at the trench. Placing one station on the downgoing plate and another on the hanging wall close to the trench may allow detection of this step while also providing critical information about the downgoing plate velocity, which is often lacking. However, the placement of the instruments is critical to avoid local effects due to thrust ramps that may impede free slip, and which are almost always present at the front of accreting wedges (e.g., Becel et al., 2017; Gulick et al., 2004; Moore et al., 1990). Transverse faults that cross the wedge could also significantly impact site velocities. Finally, seafloor geodetic data obtained during the coseismic period could constrain the dynamic aspect of the shallow fault system and help separate its coseismic and postseismic behavior.

5. Conclusions

We have quantified the creep rate of a shallow unlocked megathrust located in the stress shadow of a deeper locked portion of the fault. The creep rate near the trench is in all cases low, and relatively insensitive to the assumed width of shallow frictional unlocking. Our results, which are based on the stress state of a convergent margin, stand in contrast with the majority of purely kinematic models that do not take into account

stresses and predict creep up to the plate rate at the fault tip. We show that models assuming full shallow creep require a nonphysical tensional driving force in the accretionary wedge. Even in cases where geodetic data are available close to the trench, limited information can be inferred about the frictional properties of the fault, as a fault patch located within a stress shadow lacks the driving force needed to slip and thereby reveal its properties. Areas with spatially variable or absent deep locked patches may be sites of increased shallow creep and are key targets for future seafloor geodetic observations.

Acknowledgments
This research is supported by the National Research Foundation of Singapore and the Singapore Ministry of Education under the Research Centres of Excellence initiative and its Singapore NRF Fellowship scheme (National Research Fellow award NRF-NRFF2013-06). This work comprises Earth Observatory of Singapore contribution 192. We acknowledge Jack Loveless and an anonymous reviewer for helpful reviews that improved the quality and clarity of this manuscript. All data are available from sources cited in the reference section.

References

Abercrombie, R. E., Antolik, M., Felzer, K., & Ekström, G. (2001). The 1994 java tsunami earthquake: Slip over a subducting seamount. *Journal of Geophysical Research*, *106*(B4), 6595–6607. https://doi.org/10.1029/2000JB900403

Ader, T., Avouac, J.-P., Liu-Zeng, J., Lyon-Caen, H., Bollinger, L., Galetzka, J., et al. (2012). Convergence rate across the Nepal Himalaya and interseismic coupling on the Main Himalayan Thrust: Implications for seismic hazard. *Journal of Geophysical Research*, *117*, B04403. https://doi.org/10.1029/2011JB009071

Ammon, C. J., Kanamori, H., Lay, T., & Velasco, A. A. (2006). The 17 July 2006 Java tsunami earthquake. *Geophysical Research Letters*, *33*(24), L24308. https://doi.org/10.1029/2006GL028005

Becel, A., Shillington, D. J., Delescluse, M., Nedimović, M. R., Abers, G. A., Saffer, D. M., et al. (2017). Tsunamigenic structures in a creeping section of the Alaska subduction zone. *Nature Geoscience*, *10*(8), 609–613. https://doi.org/10.1038/NGEO2990

Bettinelli, P., Avouac, J.-P., Flouzat, M., Jouanne, F., Bollinger, L., Willis, P., & Chitrakar, G. R. (2006). Plate motion of India and interseismic strain in the Nepal Himalaya from GPS and DORIS measurements. *Journal of Geodesy*, *80*(8-11), 567–589. https://doi.org/10.1007/s00190-006-0030-3

Bilek, S., & Lay, T. (2002). Tsunami earthquakes possibly widespread manifestations of frictional conditional stability. *Geophysical Research Letters*, *29*(14), 1673. https://doi.org/10.1029/2002GL015215

Blanpied, M. L., Lockner, D. A., & Byerlee, J. D. (1995). Frictional slip of granite at hydrothermal conditions. *Journal of Geophysical Research*, *B7*, 13,045–13,064.

Bradley, K. E., Feng, L., Hill, E. M., Natawidjaja, D. H., & Sieh, K. (2017). Implications of the diffuse deformation of the Indian Ocean lithosphere for slip partitioning of oblique plate convergence in Sumatra. *Journal of Geophysical Research: Solid Earth*, *122*, 572–591. https://doi.org/10.1002/2016JB013549

Bürgmann, R., Kogan, M. G., Steblov, G. M., Hilley, G., Levin, V. E., & Apel, E. (2005). Interseismic coupling and asperity distribution along the Kamchatka subduction zone. *Journal of Geophysical Research*, *110*, B07405. https://doi.org/10.1029/2005JB003648

Byrne, D. E., Davis, D. M., & Sykes, L. R. (1988). Loci and maximum size of thrust earthquakes and the mechanics of the shallow region of subduction zones. *Tectonics*, *7*, 833–857. https://doi.org/10.1029/TC007i004p00833

Chlieh, M., Avouac, J.-P., Sieh, K., Natawidjaja, D. H., & Galetzka, J. (2008). Heterogeneous coupling of the Sumatran megathrust constrained by geodetic and paleogeodetic measurements. *Journal of Geophysical Research*, *113*, B05305. https://doi.org/10.1029/2007JB004981

Chlieh, M., Mothes, P. A., Nocquet, J.-M., Jarrin, P., Charvis, P., Cisneros, D., et al. (2014). Distribution of discrete seismic asperities and aseismic slip along the Ecuadorian megathrust. *Earth and Planetary Science Letters*, *400*, 292–301. https://doi.org/10.1016/j.epsl.2014.05.027

Chlieh, M., Perfettini, H., Tavera, H., Avouac, J.-P., Remy, D., Nocquet, J.-M., et al. (2011). Interseismic coupling and seismic potential along the Central Andes subduction zone. *Journal of Geophysical Research*, *116*, B12405. https://doi.org/10.1029/2010JB008166

Copley, A., & Reynolds, K. (2014). Imaging topographic growth by long-lived postseismic afterslip at Sefidabeh, East Iran. *Tectonics*, *33*, 330–345. https://doi.org/10.1002/2013TC003462

Davis, D., Suppe, J., & Dahlen, F. A. (1983). Mechanics of fold-and-thrust belts and accretionary wedges. *Journal of Geophysical Research*, *88*, 1153–1172. https://doi.org/10.1029/JB088iB02p01153

DeMets, C., Gordon, R. G., & abd Argus, D. F. (2010). Geologically current plate motions. *Geophysical Journal International*, *181*(1), 1–80. https://doi.org/10.1111/j.1365-246X.2009.04491.x

Denolle, M. A., Fan, W., & Shearer, P. M. (2015). Dynamics of the 2015 *M*7.8 Nepal earthquake. *Geophysical Research Letters*, *42*(18), 7467–7475. https://doi.org/10.1002/2015GL065336

Dieterich, J. H. (1981). Constitutive properties of faults with simulated gouge. In N. L. Carter, M. Friedman, J. M. Logan, & D. W. Sterns (Eds.), *Mechanical behavior of crustal rocks*, *American Geophysical Union Monograph* (Vol. 24, pp. 103–120). Washington, DC: American Geophysical Union.

Fitch, T. J., & Scholz, C. H. (1971). Mechanism of underthrusting in southwest Japan: A model of convergent plate interactions. *Journal of Geophysical Research*, *76*(29), 7260–7292. https://doi.org/10.1029/JB076i029p07260

Gagnon, K., Chadwell, C. D., & Norabuena, E. (2005). Measuring the onset of locking in the Peru–Chile trench with GPS and acoustic measurements. *Nature*, *434*(7030), 205–208. https://doi.org/10.1038/nature03412

Geersen, J., Ranero, C. R., Kopp, H., Behrmann, J. H., Lange, D., Klaucke, I., et al. (2018). Does permanent extensional deformation in lower forearc slopes indicate shallow plate-boundary rupture? *Earth and Planetary Science Letters*, *489*, 17–27. https://doi.org/10.1016/j.epsl.2018.02.030

Grandin, R., Doin, M.-P., Bollinger, L., Pinel-Puyssegur, B., Ducret, G., Jolivet, R., et al. (2012). Long-term growth of the Himalaya inferred from interseismic InSAR measurement. *Geology*, *40*, 105–1062. https://doi.org/10.1130/G33154.1

Grevemeyer, I., & Tiwari, V. M. (2006). Overriding plate controls spatial distribution of large thrust earthquakes in the Sunda-Andaman subduction zone. *Earth and Planetary Science Letters*, *251*(3-4), 199–208. https://doi.org/10.1016/j.epsl.2006.08.021

Gulick, S. P. S., Bangs, N. L. B., Shipley, T. H., Nakamura, Y., Moore, G., & Kuramoto, S. (2004). Three-dimensional architecture of the Nankai accretionary prism's imbricate thrust zone off Cape Muroto, Japan: Prism reconstruction via en echelon thrust propagation. *Journal of Geophysical Research*, *109*, B02105. https://doi.org/10.1029/2003JB002654

Hayes, G. P., Wald, D. J., & Johnson, R. L. (2012). Slab1.0: A three-dimensional model of global subduction zone geometries. *Journal of Geophysical Research*, *117*, B01302. https://doi.org/10.1029/2011JB008524

Herman, F., Copeland, P., Avouac, J.-P., Bollinger, L., Maheo, G., Le Fort, P., et al. (2010). Exhumation, crustal deformation, and thermal structure of the Nepal Himalaya derived from the inversion of thermochronological and thermobarometric data and modeling of the topography. *Journal of Geophysical Research*, *115*, B06407. https://doi.org/10.1029/2008JB006126

Hetland, E., & Simons, M. (2010). Post-seismic and interseismic fault creep II: Transient creep and interseismic stress shadows on megathrusts. *Geophysical Journal International*, *181*(1), 99–112. https://doi.org/10.1111/j.1365-246X.2009.04482.x

Hill, E. M., Borrero, J. C., Hiang, Z., Qui, Q., Banerjee, P., Natawidjaja, D. H., et al. (2012). The 2010 Mw 7.8 Mentawai earthquake: Very shallow source of a rare tsunami earthquake determined from tsunami field survey and near-field GPS data. *Journal of Geophysical Research*, *117*, B06402. https://doi.org/10.1029/2012JB009159

Huang, Y., Meng, L., & Ampuero, J. P. (2012). A dynamic model of the frequency-dependent rupture process of the 2011 Tohoku-Oki earthquake. *Earth, Planets and Space*, *64*(12), 1061–1066. https://doi.org/10.5047/eps.2012.05.011

Hubbard, J., Barbot, S., Hill, E. M., & Tapponnier, P. (2015). Coseismic slip on shallow décollement megathrusts: Implications for seismic and tsunami hazard. *Earth Science Reviews*, *141*, 45–55. https://doi.org/10.1016/j.earscirev.2014.11.003

Hyndman, R. D. (2013). Downdip landward limit of Cascadia great earthquake rupture. *Journal of Geophysical Research: Solid Earth*, *118*, 5530–5549. https://doi.org/10.1002/jgrb.50390

Hyndman, R. D., & Wang, K. (1993). Thermal constraints on the zone of major thrust earthquake failure: The Cascadia subduction zone. *Journal of Geophysical Research*, *98*(B2), 2039–2060. https://doi.org/10.1029/92JB02279

Hyndman, R. D., Yamano, M., & Oleskevich, D. A. (1997). The seismogenic zone of subduction thrust faults. *The Island Arc*, *6*(3), 244–260. https://doi.org/10.1111/j.1440-1738.1997.tb00175.x

Ide, S., Baltay, A., & Beroza, G. (2011). Shallow dynamic overshoot and energetic deep rupture in the 2011 Mw 9.0 Tohoku-Oki earthquake. *Science*, *332*(6036), 1426–1429. https://doi.org/10.1126/science.1207020

Ikari, M. J., Saffer, D. M., & Marone, C. (2009). Frictional and hydrologic properties of clay-rich fault gouge. *Journal of Geophysical Research*, *114*, B05409. https://doi.org/10.1029/2008JB006089

Jackson, M., & Bilham, R. (1994). Constraints on Himalayan deformation inferred from vertical velocity fields in Nepal and Tibet. *Journal of Geophysical Research*, *99*, 13,897–13,912. https://doi.org/10.1029/94JB00714

Kaneko, Y., Avouac, J.-P., & Lapusta, N. (2010). Towards inferring earthquake patterns from geodetic observations of interseismic coupling. *Nature Geoscience*, *3*(5), 363–369. https://doi.org/10.1038/ngeo843

Kido, M., Osada, Y., Fujimoto, H., Hino, R., & Ito, Y. (2011). Trench-normal variation in observed seafloor displacements associated with the 2011 Tohoku-Oki earthquake. *Geophysical Research Letters*, *38*, L24303. https://doi.org/10.1029/2011GL050057

Kodaira, S., No, T., Nakamura, Y., Fujiwara, T., Kaiho, Y., Miura, S., et al. (2012). Coseismic fault rupture at the trench axis during the 2011 Tohoku-oki earthquake. *Nature Geoscience*, *5*(9), 646–650. https://doi.org/10.1038/ngeo1547

Konca, A. O., Avouac, J.-P., Sladen, A., Meltzner, A. J., Sieh, K., Fang, P., et al. (2008). Partial rupture of a locked patch of the Sumatra megathrust during the 2007 earthquake sequence. *Nature*, *456*(7222), 631–635. https://doi.org/10.1038/nature07572

Kreemer, C., Klein, E., Shen, Z.-K., Wang, M., Estey, L., Wier, S., et al. (2014). A geodetic plate motion and Global Strain Rate Model. *Geochemistry, Geophysics, Geosystems*, *15*(10), 3849–3889. https://doi.org/10.1002/2014GC005407

Lay, T., & Kanamori, H. (1981). An asperity model of large earthquake sequences. In D. W. Simpson & P. G. Richards (Eds.), *Earthquake prediction, and international review*, *Maurice Ewing series* (Vol. IV, pp. 579–592). Washington, DC: American Geophysical Union.

Lay, T., Kanamori, H., Ammon, C. J., Koper, K. D., Hutko, A. R., Ye, L., et al. (2012). Depth-varying rupture properties of subduction zone. *Journal of Geophysical Research*, *117*, B04311. https://doi.org/10.1029/2011JB009133

Lay, T., & Schwarz, S. (2004). Comment on "Coupling semantics and science in earthquake research". *Eos*, *85*(36), 339–340. https://doi.org/10.1029/2004EO360003

Li, S., Moreno, M., Rosenau, M., Melnick, D., & Oncken, O. (2014). Splay fault triggering by great subduction earthquakes inferred from finite element models. *Geophysical Research Letters*, *41*, 385–391. https://doi.org/10.1002/2013GL058598

Loveless, J. P., & Meade, B. J. (2010). Geodetic imaging of plate motions, slip rates, and partitioning of deformation in Japan. *Journal of Geophysical Research*, *115*, B02410. https://doi.org/10.1029/2008JB006248

Loveless, J. P., & Meade, B. J. (2011). Spatial correlation of interseismic coupling and coseismic rupture extent of the 2011 M_W = 9.0 Tohoku-oki earthquake. *Geophysical Research Letters*, *38*, L17306. https://doi.org/10.1029/2011GL048561

Loveless, J. P., & Meade, B. J. (2016). Two decades of spatiotemporal variations in subduction zone coupling offshore Japan. *Earth and Planetary Science Letters*, *436*, 19–30. https://doi.org/10.1016/j.epsl.2015.12.033

Marone, C. (1998). Laboratory-derived friction laws and their application to seismic faulting. *Annual Review of Earth and Planetary Sciences*, *26*(1), 643–696. https://doi.org/10.1146/annurev.earth.26.1.643

Marone, C., & Scholz, C. H. (1988). The depth of seismic faulting and the upper transition from stable to unstable slip regimes. *Geophysical Research Letters*, *15*(6), 621–624. https://doi.org/10.1029/GL015i006p00621

McCaffrey, R. (1991). Slip vectors and stretching of the Sumatran fore arc. *Geology*, 19,881–19,884.

McCaffrey, R. (2014). Interseismic locking on the Hikurangi subduction zone: Uncertainties from slow-slip events. *Journal of Geophysical Research*, *119*, 7874–7888. https://doi.org/10.1002/2014JB010945

Mencin, D., Bendick, R., Upreti, B. N., Adhikari, D. P., Gajurel, A. P., Bhattarai, R. R., et al. (2016). Himalayan strain reservoir inferred from limited afterslip following the Gorkha earthquake. *Nature Geoscience*, *9*(7), 533–537. https://doi.org/10.1038/NGEO2734

Metois, M., Socquet, A., Vigny, C., Carrizo, D., Peyrat, S., Delorme, A., et al. (2013). Revisiting the North Chile seismic gap segmentation using GPS-derived interseismic coupling. *Geophysical Journal International*, *194*(3), 1283–1294. https://doi.org/10.1093/gji/ggt183

Moore, G. F., Shipley, T. H., Stoffa, P. L., Karig, D. E., Taira, A., Kuramoto, S., et al. (1990). Structure of the Nankai Trough accretionary zone from multichannel seismic reflection data. *Journal of Geophysical Research*, *95*, 8573–8765.

Moore, J. C., & Saffer, D. M. (2001). Updip limit of the seismogenic zone beneath the accretionary prism of southwest Japan: An effect of diagenetic to low-grade metamorphic processes and increasing effective stress. *Geology*, *29*(2), 183–186. https://doi.org/10.1130/0091-7613(2001)029%3C0183:ULOTSZ%3E2.0.CO;2

Moreno, M., Haberland, C., Oncken, O., Rietbrock, A., Angiboust, S., & Heidbach, O. (2014). Locking of the Chile subduction zone controlled by fluid pressure before the 2010 earthquake. *Nature Geoscience*, *7*(4), 292–296. https://doi.org/10.1038/NGEO2102

Moreno, M., Rosenau, M., & Oncken, O. (2010). 2010 Maule earthquake slip correlates with pre-seismic locking of Andean subduction zone. *Nature*, *467*(7312), 198–202. https://doi.org/10.1038/nature09349

Nocquet, J.-M., Jarrin, P., Vallee, M., Mothes, P. A., Grandin, R., Rolandone, F., et al. (2017). Supercycle at the Ecuadorian subduction zone revealed after the 2016 Pedernales earthquake. *Nature Geoscience*, *10*(2), 145–149. https://doi.org/10.1038/NGEO2864

Okada, Y. (1992). Internal deformation due to shear and tensile faults in a half space. *Bulletin of the Seismological Society of America*, *82*, 1018–1040.

Pandey, M. R., Tandukar, R. P., Avouac, J.-P., Lave, J., & Massot, J. P. (1995). Interseismic strain accumulation on the Himalayan crustal ramp (Nepal). *Geophysical Research Letters*, *22*(7), 751–754. https://doi.org/10.1029/94GL02971

Perfettini, H., Avouac, J. P., Tavera, H., Kositsky, A., Nocquet, J. M., Bondoux, F., & Soler, P. (2010). Seismic and aseismic slip on the Central Peru megathrust. *Nature*, *465*(7294), 78–81. https://doi.org/10.1038/nature09062

Ruina, A. (1983). Slip instability and state variable friction laws. *Journal of Geophysical Research*, *88*(B12), 10,359–10,370. https://doi.org/10.1029/JB088iB12p10359

Saffer, D. M. (2017). Mapping fluids to subduction megathrust locking and slip behavior. *Geophysical Research Letters*, *44*, 9337–9340. https://doi.org/10.1002/2017GL075381

Saffer, D. M., & Wallace, L. M. (2015). The frictional, hydrologic, metamorphic and thermal habitat of shallow slow earthquakes. *Nature Geoscience*, *8*(8), 594–600. https://doi.org/10.1038/NGEO2490

Savage, J. C. (1983). A dislocation model of strain accumulation and release at a subduction zone. *Journal of Geophysical Research*, *88*(B6), 4984–4996. https://doi.org/10.1029/JB088iB06p04984

Schmalzle, G. M., McCaffrey, R., & Creager, K. (2014). Central Cascadia subduction zone creep. *Geochemistry, Geophysics, Geosystems*, *15*(4), 1515–1532. https://doi.org/10.1002/2013GC005172

Scholz, C. H. (1988). The brittle-plastic transition and the depth of seismic faulting. *Geologische Rundschau*, *77*, 39–328.

Scholz, C. H. (1998). Earthquakes and friction laws. *Nature*, *391*(6662), 37–42. https://doi.org/10.1038/34097

Scholz, C. H., & Campos, J. (1995). On the mechanism of seismic decoupling and back arc spreading at subduction zones. *Journal of Geophysical Research*, *100*(B11), 22,103–22,115. https://doi.org/10.1029/95JB01869

Schwarz, S., & DeShon, H. (2007). Distinct updip limits to geodetic locking and microseismicity at the Northern Costa Rican seismogenic zone. In T. Dixon & J. C. Moore (Eds.), *The seismogenic zone of subduction thrust faults* (pp. 576–599). New York: Columbia University Press. https://doi.org/10.7312/dixo13866-018

Stesky, R. M., Brace, W. F., Riley, D. K., & Robin, P.-Y. F. (1974). Friction in faulted rock at high temperature and pressure. *Tectonophysics*, *23*(1-2), 177–203. https://doi.org/10.1016/0040-1951(74)90119-X

Stevens, V. L., & Avouac, J. P. (2015). Interseismic coupling on the Main Himalayan Thrust. *Geophysical Research Letters*, *42*, 5828–5837. https://doi.org/10.1002/2015GL064845

Sun, T., Wang, K., Fujiwara, T., Kodaira, S., & He, J. (2017). Large fault slip peaking at trench in the 2011 Tohoku-oki earthquake. *Nature Communications*, *8*. https://doi.org/10.1038/ncomms14044

Syracuse, E. M., van Keken, P. E., & Abers, G. A. (2010). The global range of subduction zone thermal models. *Physics of the Earth and Planetary Interiors*, *183*(1-2), 73–90. https://doi.org/10.1016/j.pepi.2010.02.004

Tichelaar, B. W., & Ruff, L. J. (1993). Depth of seismic coupling along subduction zones. *Journal of Geophysical Research*, *98*(B2), 2017–2037. https://doi.org/10.1029/92JB02045

Vrolijk, P. (1990). On the mechanical role of smectite in subduction zones. *Geology*, *18*(8), 703–707. https://doi.org/10.1130/0091-7613(1990)018%3C0703:OTMROS%3E2.3.CO;2

Wallace, L. M., Kaneko, Y., Hreinsdottir, S., Hamling, I., Peng, Z., Bartlow, N., et al. (2017). Large-scale dynamic triggering of shallow slow slip enhanced by overlying sedimentary wedge. *Nature Geoscience*, *10*(10), 765–770. https://doi.org/10.1038/NGEO3021

Wallace, L. M., Webb, S. C., Ito, Y., Mochizuki, K., Hino, R., Henrys, S., et al. (2016). Slow slip near the trench at the Hikurangi subduction zone, New Zealand. *Science*, *352*(6286), 701–704. https://doi.org/10.1126/science.aaf2349

Wang, K., & Dixon, T. (2004). "Coupling" semantics and science in earthquake research. *Eos*, *85*(18), 180–181. https://doi.org/10.1029/2004EO180005

Wu, F. T., Blatter, L., & Roberson, H. (1975). Clay gouges in the San Andreas Fault System and their possible implications. In M. Wyss (Ed.), *Earthquake prediction and rock mechanics*, *Contributions to Current Research in Geophysics (CCRG)* (pp. 87–95). Basel: Birkhäuser. https://doi.org/10.1007/978-3-0348-5534-1_8

Xu, S., Fukuyama, E., Yue, H., & Ampuero, J.-P. (2016). Simple crack models explain deformation induced by subduction zone megathrust earthquakes. *Bulletin of the Seismological Society of America*, *106*(5), 2275–2289. https://doi.org/10.1785/0120160079

Xue, L., Schwartz, S., Liu, Z., & Feng, L. (2015). Interseismic megathrust coupling beneath the Nicoya Peninsula, Costa Rica, from the joint inversion of InSAR and GPS data. *Journal of Geophysical Research: Solid Earth*, *120*, 3707–3722. https://doi.org/10.1002/2014JB011844

Yao, H., Shearer, P. M., & Gerstoft, P. (2013). Compressive sensing of frequency-dependent seismic radiation from subduction zone megathrust ruptures. *Proceedings of the National Academy of Sciences of the United States of America*, *110*(12), 4512–4517. https://doi.org/10.1073/pnas.1212790110

Yokota, Y., Ishikawa, T., Watanabe, S.-I., Tashiro, T., & Asada, A. (2016). Seafloor geodetic constraints on interplate coupling of the Nankai trough megathrust zone. *Nature*, *534*(7607), 374–377. https://doi.org/10.1038/nature17632

Yue, H., Lay, T., Rivera, L., Bai, Y., Yamazaki, Y., Cheung, K. F., et al. (2014). Rupture process of the 2010 M_w 7.8 Mentawai tsunami earthquake from joint inversion of near-field hr-GPS and teleseismic body wave recordings constrained by tsunami observations. *Journal of Geophysical Research: Solid Earth*, *119*, 5574–5593. https://doi.org/10.1002/2014JB011082

Yue, H., Simons, M., Duputel, Z., Jiang, J., Fielding, E., Liang, C., et al. (2016). Depth varying rupture properties during the 2015 Mw 7.8 Gorkha (Nepal) earthquake. *Tectonophysics*, *714-715*, 44–54. https://doi.org/10.1016/j.tecto.2016.07.005

Zhao, B., Burgmann, R., Wang, D., Tan, K., Du, R., & Zhang, R. (2017). Dominant controls of downdip afterslip and viscous relaxation on the Postseismic displacements following the M_w7.9 Gorkha, Nepal, earthquake. *Journal of Geophysical Research: Solid Earth*, *122*, 8376–8401. https://doi.org/10.1002/2017JB014366